OTC 20912

Uplift Resistance of Buried Pipelines at Low Cover-Diameter Ratios

J. Wang, R. Ahmed, S.K. Haigh, University of Cambridge; N.I. Thusyanthan, S. Mesmar, KW Ltd

Copyright 2010, Offshore Technology Conference

This paper was prepared for presentation at the 2010 Offshore Technology Conference held in Houston, Texas, USA, 3–6 May 2010.

This paper was selected for presentation by an OTC program committee following review of information contained in an abstract submitted by the author(s). Contents of the paper have not been reviewed by the Offshore Technology Conference and are subject to correction by the author(s). The material does not necessarily reflect any position of the Offshore Technology Conference, its officers, or members. Electronic reproduction, distribution, or storage of any part of this paper without the written consent of the Offshore Technology Conference is prohibited. Permission to reproduce in print is restricted to an abstract of not more than 300 words; illustrations may not be copied. The abstract must contain conspicuous acknowledgment of OTC copyright.

Abstract

Reliable estimates for the maximum available uplift resistance from the backfill soil are essential to prevent upheaval buckling of buried pipelines. The current design code DNV RP F110 does not offer guidance on how to predict the uplift resistance when the cover:pipe diameter (H/D) ratio is less than 2. Hence the current industry practice is to discount the shear contribution from uplift resistance for design scenarios with H/D ratios less than 1. The necessity of this extra conservatism is assessed through a series of full-scale and centrifuge tests, 21 in total, at the Schofield Centre, University of Cambridge. Backfill types include saturated loose sand, saturated dense sand and dry gravel. Data revealed that the Vertical Slip Surface Model remains applicable for design scenarios in loose sand, dense sand and gravel with H/D ratios less than 1, and that there is no evidence that the contribution from shear should be ignored at these low H/D ratios. For uplift events in gravel, the shear component seems reliable if the cover is more than 1-2 times the average particle size (D_{50}), and more research effort is currently being carried out to verify this conclusion. Strain analysis from the Particle Image Velocimetry (PIV) technique proves that the Vertical Slip Surface Model is a good representation of the true uplift deformation mechanism in loose sand at H/D ratios between 0.5 and 3.5. At very low H/D ratios (H/D < 0.5), the deformation mechanism is more wedge-like, but the increased contribution from soil weight is likely to be compensated by the reduced shear contributions. Hence the design equation based on the Vertical Slip Surface Model still produces good estimates for the maximum available uplift resistance. The evolution of shear strain field from PIV analysis provides useful insight into how uplift resistance is mobilized as the uplift event progresses. The output of this research leads to significant savings, especially for larger diameter pipelines, on rock tonnage which is required to mitigate upheaval buckling.

Introduction

Pipeline networks are instrumental for transporting hot crude oil from offshore platforms to onshore refineries. At shallow water sites (water depth ≤15 metres), the trench-and-burial method is typically adopted for pipeline laying projects, and the excavated material during trenching is used as primary backfill. The purpose of burial is three-fold: Firstly, the soil cover shields the pipeline from physical damages such as collisions, trawl-gear and anchor operations; Secondly, the surrounding soil provides additional thermal insulation, and helps maintain the high temperature in the containment required for low-viscosity crude oil flow; Last but not least, the overlying soil resists any tendency of the pipeline to move vertically upwards, the result of a phenomenon known as upheaval buckling (UHB).

UHB is a thermally induced structural effect. The operating conditions of high temperature and large internal pressure, which are significantly above the ambient seabed conditions at first laying, lead to thermal extensions of the pipeline. These axial movements are restricted by the frictional forces at the soil-pipeline interface. Consequently, large compressive forces are developed throughout the pipeline profile, which can cause it to buckle globally if restricting forces are inadequate. At locations where the pipeline profile features an over-bend, the easiest mode of buckling is for the pipeline to heave upwards through the backfill soil, hence the name upheaval buckling. For safe design at these locations, the upward heaving force generated by UHB must be adequately balanced by the downward resistance provided by the cover. Wherever this resistance is inadequate, an additional layer of rock dump will be required as secondary backfill.

For offshore pipeline projects, the installation process and any subsequent remedial measures are costly. Hence reliable estimates of the required trenching depths and cover heights are highly desirable. Present understanding of soil resistance to UHB, or uplift resistance, is based on analyses and experimental work (Vesic, 1971; Rowe and Davis, 1982; Hobbs, 1984; Randolph and Houlsby, 1984; Trautman *et al*., 1985; Palmer *et al*., 1990; Schaminée *et al*., 1990; Dickin, 1994; Croll, 1997; Moradi and Craig, 1998; Baumgard, 2000; White *et al*., 2001; Bransby *et al*., 2001; and Cheuk, 2005) by researchers on both structural and geotechnical fronts. Most research effort has been conducted in granular soils and at medium cover-pipe

diameter ratios (H/D ≥ 2, where H is the vertical distance between the cover surface and the pipe crown, and D is the external diameter of the pipeline). In actual offshore projects and for large-diameter pipelines in particular, actual burial depths are often equivalent to H/D ratios between 0.5 and 2.0, and there is a lack of experimental data for this region.

The current design practice for uplift resistance with low H/D ratios is more empirical than analytical. Improved design efficiency would arise from a better understanding of the deformation mechanism above an uplifting pipe, and hence a better basis for calculating the variation of uplift resistance with respect to pipe upward displacement. Small-scale model tests are widely used to evaluate uplift resistance. Comparison between model and full-scale experiments shows good agreement with respect to peak uplift resistance, but there are significant discrepancies in the mobilisation displacement when expressed dimensionlessly (Palmer et al., 2003). Other notable puzzles include pipe ratcheting, the effect of the degree of consolidation of backfill, partial backfill disturbance due to trenching, the effect of rock-dump and the effect of pull-up rate on the uplift resistance in both sandy and clayey backfills.

A series of both full scale (1g) and centrifuge (30g) experiments have been conducted at the Schofield Centre, University of Cambridge, to model the uplift response of pipelines buried in saturated sand and dry gravel at low H/D ratios (H/D ≤ 2). The results have shown that design confidence can be improved by acknowledging shear contributions to the total available uplift resistance in both sand and gravel at low H/D ratios. The Particle Image Velocimetry technique has been employed to reveal the actual deformation mechanism invoked in the uplift process. This research paper will elaborate on these findings.

Literature Review

The structural aspects of the UHB problem are well understood. The UHB stability of the pipeline is governed by force balance between the axial compressive force *P* and the available downward restraints (Timoshenko and Goodier, 1934). The general solution is of the form (Palmer et al., 1990):

$$\Phi_w = A\left(\frac{\pi}{\Phi_L}\right)^2 - B\left(\frac{\pi}{\Phi_L}\right)^4 \qquad \text{Equation 1}$$

where $\Phi_w = \frac{wEI}{\delta P^2}$ is the dimensionless uplift resistance; $\Phi_L = L\sqrt{\frac{P}{EI}}$ is the dimensionless imperfection length; EI is the flexural rigidity of the pipeline; P is the thermally-generated axial compressive force; δ is the maximum height of the imperfection; L is half the total imperfection length; And A, B are constants to be determined numerically. The solution for any particular pipeline section will depend on the initial imperfection profile (Croll, 1997). As Φ_w intrinsically depends upon δ, any additional upward movement of the pipeline would act as feedback into calculation. Hence the exact equilibrium is also related to how the available uplift resistance is mobilised as the pipeline moves upwards through the soil cover.

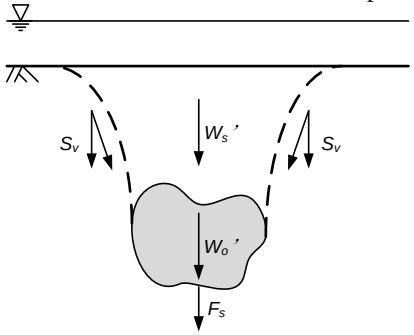

Figure 1: Generalised components of uplift resistance for an object buried in seabed

The initial breakout resistance of objects embedded underground consists of four components[1] (Versic, 1971), as illustrated in Figure 1:

1. The submerged effective weight of the object, W'_o
2. The submerged effective weight of soil being lifted, W'_s
3. The vertical component of the soil shearing resistance, S_v
4. The vertical component of the suction force due to excess pore pressure differences above and below the object, F_s

For pipeline UHB design, the W'_o term can be accurately assessed and is independent of cover conditions. The contribution from F_s depends directly on the pull-out speed (Thusyanthan et al., 2008, Bransby and Ireland, 2009, and Wang et al., 2009); hence it is sufficient and conservative to assume fully drained scenarios. Therefore, the contribution from the cover soil is the sum of W'_s and S_v only. This "true" uplift resistance depends on the deformation mechanism as well as properties of the soil.

In cohesionless soils, one popular hypothetical mechanism is the "Vertical Slip Surface" model with linearly varying

[1] Versic, (1971) includes a fifth component as the adhesion between the object and the adjacent soil. Schofield and Wroth, (1968) suggests that adhesion arises from negative pore water pressures during soil dilation, hence is indistinguishable from F_s.

shear resistance with increased depth (Trautman et al., 1985), as illustrated in Figure 2. The peak "true" uplift resistance per unit length, R_{peak}, can be derived from equilibrium in the vertical direction (Pederson and Jensen, 1988):

$$\frac{R_{peak}}{\gamma' H D} = 1 + 0.1\frac{D}{H} + f_p\left[\frac{D}{H} \times \left(\frac{H}{D} + \frac{1}{2}\right)^2\right] \quad \text{Equation 2}$$

where f_p is the dimensionless Pederson Uplift Factor. At high H/D ratios (H/D > 6), Equation 3 can be further simplified by ignoring the second term and lower-order H/D terms (Schaminée et al., 1990):

$$\frac{R_{peak}}{\gamma' H D} = 1 + f_s\frac{H}{D} \quad \text{Equation 3}$$

where f_s is the Schaminée uplift resistance factor for cohesionless soils. For UHB in medium to dense sandy backfill, the Inclined Slip Surface Model, which employs the dilatancy of the soil, is experimentally proven (White et al, 2001) to be a closer approximation to the real deformation mechanism. However, the design equation derived from this model is algebraically indistinguishable from Equation 2 (Thusyanthan et al., 2010).

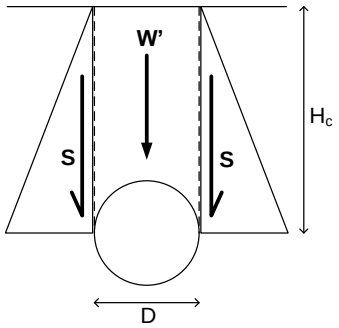

Figure 2: The Vertical Slip Surface Model

Current Design Practice

The current design practice for uplift resistance in cohesionless soils (sands and gravels) is based on Equation 2 (DNV-RP-F110). Suggested values for f_p and the applicable H/D range are summarised in Table 1. The limited range of H/D ratios applicable in each case is particularly worth noting. As the DNV guideline does not specify a design method for scenarios with low H/D ratios, the commonly accepted current practice is to ignore the contribution from shear altogether when H/D ratios are below 1, i.e., forcing $f_p = 0$ and limiting R_{peak} to the weight of the soil cover alone:

$$\frac{R_{peak}}{\gamma' HD} = 1 \quad \text{(for H/D < 1)} \quad \text{Equation 4}$$

Table 1: Suggested f_p values in DNV guideline

Backfill Type	ϕ_{peak} (°)	*H/D Range*	Mean f_p	Range of f_p
Loose Sand	30	[3.5, 7.5]	0.29	[0.1, 0.3]
Medium Sand	35	[2.0, 8.0]	0.47	[0.4, 0.6]
Dense Sand	40	[2.0, 8.0]	0.62	
Rock	N/A	[2.0, 8.0]	0.62	[0.5, 0.8]

This extra-conservatism at low H/D ratios can lead to large quantities of rock dump material being required as secondary backfill, which can cost millions of dollars. The major reason behind this conservatism is the absence of available data at these low H/D ratios.

Research Objectives

Theoretically, it is a natural assumption that shear should still contribute towards the total "true" uplift resistance at H/D ratios below 1 in the absence of any apparent change in the deformation mechanism. Hence Equation 2 should equally be applicable. This hypothesis is tested thoroughly in this research project.

A series of pipeline uplift resistance tests have been devised and conducted in cohesionless soils at the Schofield Centre, University of Cambridge. The test series can be further divided into three categories:

1. Full scale (1g) uplift resistance testing in sand
2. Full scale (1g) uplift resistance testing in gravel
3. Centrifuge (30g) uplift resistance testing in sand

The principal objective of these tests is to understand the reliability of the shear component of the "true" uplift resistance in cohesionless soils at H/D ratios below 2, with a particular focus on H/D ratios below 1. Another parallel objective is to understand the how far the pipeline has to move in order to mobilize the peak uplift resistance, i.e. the mobilization distance. Detailed results and conclusions on this aspect are explained in Thusyanthan et al., (2010) and Wang et al., (2010).

Full Scale Testing in Sand: Apparatus and Test Program

Figure 3 shows a schematic plot and a photograph of the full-scale plane-strain test tank. It comprises two components: a container and an actuator. Both components are joined together via ten M12 bolts. The actuator is driven by a precision 250:1 stepper motor with a 40:1 direct gear box and a right-angle gearbox. The stepper motor is software controlled by a remote PC, which allows direct feedback of load cell and pore-pressure transducer (PPT) signals. This ensures that drained conditions are enforced throughout the pull-out process. A 400N tension-compression load cell connects the vertical actuator with the connector rod. The container has internal dimensions of 1000 mm (L) × 76 mm (W) × 850 mm (H). It has a steel framework, base and back to provide adequate strength in heavy-duty experiments. Its front face features a transparent Perspex cover, detachable from the frame. This enables direct observation of backfill movement and, more importantly, the possibility of using the Particle Image Velocimetry (PIV) technique to reveal the displacement field of the backfill throughout the pull-out event. Two additional pieces of laminated glass are fitted to the internal front and back faces of the container. The frictional force between the sand and glass is insignificant compared with the uplift force. A 30° foam wedge is fixed to the base of the container. Its purposes are three-fold: firstly to simulate the installation condition for the pipe after trenching; secondly to be consistent with the model container used in minidrum centrifuge modelling; and finally to save cost by reducing the amount of sand used in each test. Water infill and drainage is facilitated by a hose through the base and foam wedge, so that the backfill can be saturated from bottom up to minimise the possibility of trapping air voids.

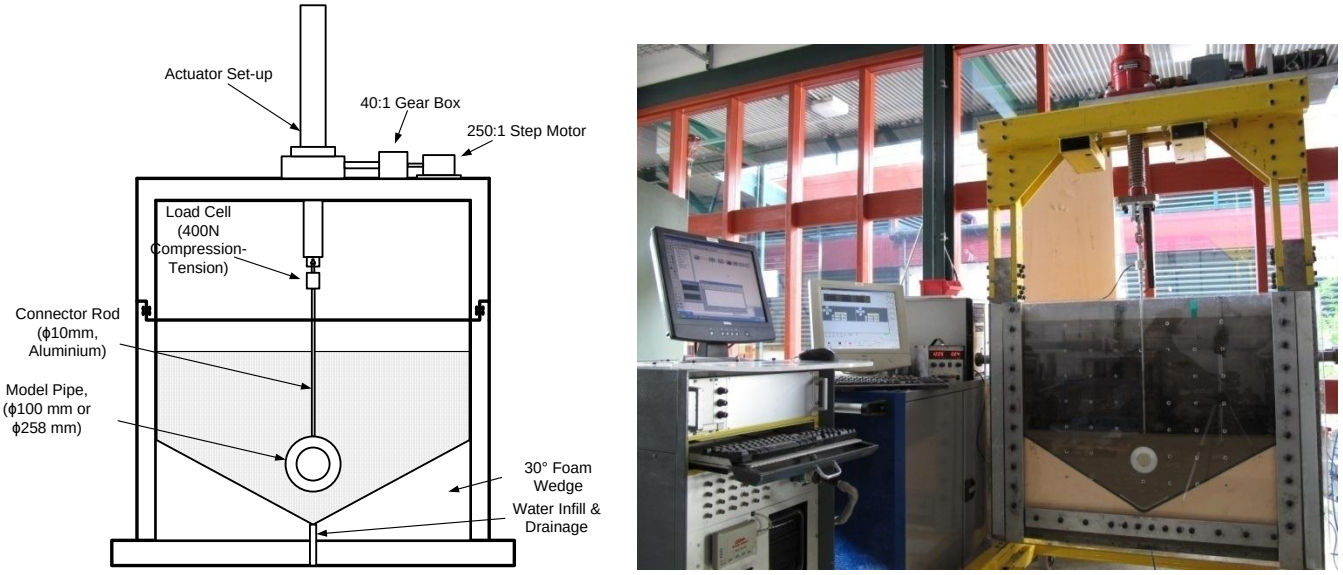

Figure 3: Full-scale plane-strain test tank in (a) schematic plot, and (b) photograph of complete set-up

Two model pipes with external diameters of 100 mm and 258 mm with PTFE front and back faces were manufactured. The PTFE material has a very low friction angle against glass, which minimises the end effects in 2D plain strain modelling. Either pipe will be connected to the actuator via a 12 mm diameter aluminium rod. The cross sectional area of the rod represents 1.03% of the projected area of the 100 mm diameter model pipe and 0.40% of the 258 mm diameter model pipe. Hence its effect on the measured uplift resistance is negligible.

Fraction E sand of relative density I_D = 35% and saturated unit weight γ_{sat} of 18.5 kN/m^3 was used as backfill, and the test was conducted in a saturated condition. The Particle Image Velocimetry (PIV) technique is utilised via a single Canon G10 digital camera to capture the displacement field of the backfill around the pipe throughout the pull-out process. The detailed test program is summarized in Table 2.

Table 2: Full scale test program for uplift resistance in sand

Test No.	Backfill	Saturated /Dry	H/D Ratio	Model Pipe Diameter (mm)	Remarks
1	Sand	Saturated	0.1	100	• Full scale tests using a small diameter model pipe • Backfill relative density I_D = 35% • All tests in saturated conditions • PIV will be used for all tests • 30° foam wedges used to simulate trenching
2	Sand	Saturated	0.3	100	
3	Sand	Saturated	0.4	100	
4	Sand	Saturated	0.5	100	
5	Sand	Saturated	1	100	
6	Sand	Saturated	2	100	
7	Sand	Saturated	3.5	100	
8	Sand	Saturated	0.5	258	• Full scale tests using a large diameter model pipe • All other conditions same as Tests No. 1 to 7
9	Sand	Saturated	1.0	258	

Full Scale Testing in Gravel: Apparatus and Test Program

All uplift resistance tests in rock were conducted within a container of dimensions 1490 mm (L) × 500 mm (W) × 895 mm (Depth). The model pipe used has an external diameter of 100 mm and a length of 500 mm. PTFE end caps were fitted to minimize frictional end effects. A motorized crane mounted on top of the container was used as the actuator, which was attached to the model pipe via a string-and-stud mechanism. All tests are conducted in dry gravel that has a D_{50} of 33 mm and mean unit weight of 18 kN/m^3. Photographs of the container and model pipe are shown in Figure 4, and the detailed test program is summarized in Table 3.

(a) (b)

Figure 4: Full-scale gravel test apparatus (a) test tank, and (b) model pipe set-up

Table 3: Full scale test program for uplift resistance in gravel

Test No.	Backfill	Saturated /Dry	H/D Ratio	Model Pipe Diameter (mm)
10	Gravel	Dry	0	100
11	Gravel	Dry	0.3	100
12	Gravel	Dry	0.5	100
13	Gravel	Dry	0.75	100
14	Gravel	Dry	1	100
15	Gravel	Dry	2	100

Centrifuge Testing: Apparatus and Test Program

As a physical modelling technique, centrifuge testing has been used extensively in pipeline uplift resistance studies. By making use of centrifugal acceleration, the centrifuge model can achieve the same stress state as that of the prototype. The strain response of the soil would then be similar, if rate effects and the influence of grain size are either allowed for or negligible. The fundamental scaling law is to ensure the same effective stress state between the model and the prototype. Centrifuge modelling principles are explained in detail by Schofield, (1980).

The 0.74 m diameter Minidrum Centrifuge at the Schofield Centre, University of Cambridge, was adopted for the second category of uplift resistance tests. This apparatus can reach 471g when spinning at the maximum speed of 1067 rpm, where g is the acceleration due to gravity (i.e. 9.81 m/s^2). Detailed configuration and features of the Minidrum Centrifuge are presented by Barker, (1998). The model set-up is illustrated schematically in Figure 5. The vertical pipe uplift movement was triggered by a radial displacement controlled actuator, which can run at constant speeds ranging from 0.002 mm/s to 0.2 mm/s and has a stroke length of 120 mm. The pipe uplift resistance was measured by two load cells mounted at the end of the actuator's moving arm. The model pipe is connected to the load cell through stainless steel wires of 0.6 mm diameter with a safe working load of 50 kg. These thin lines minimise, to a large extent, the disturbance caused to the backfill. A displacement transducer was mounted on the actuator to measure the vertical displacement. The base of the model container is made from aluminium sheet formed into a symmetrical trench with 30° side slopes. A model pipe, 8.6 mm in diameter and 120 mm in length, was used. The pipe is supported at each end on a cradle during the model preparation and consolidation phases of the test. When resting on the cradle, the bottom of the pipe is located at a distance of 0.5D above the trench base. The trench has a length of 15 mm, so the pipe is not fitted tight against the ends. The length/diameter ratio of the pipe (120 mm / 8.6 mm) is sufficiently high for end effects to be ignored.

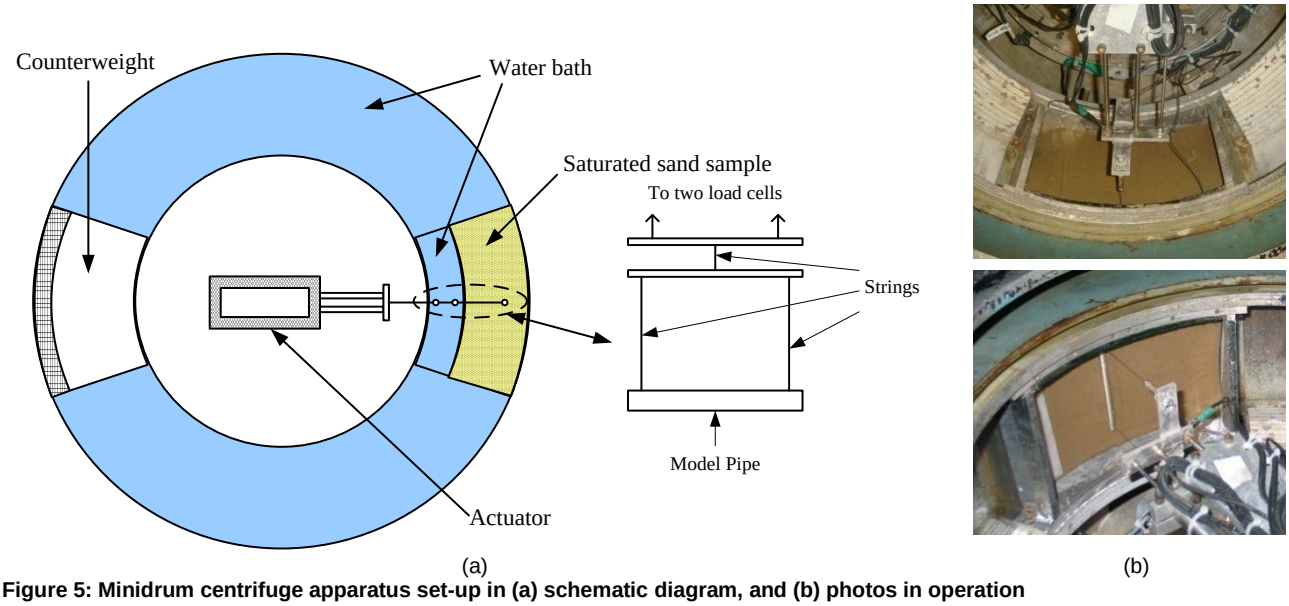

Figure 5: Minidrum centrifuge apparatus set-up in (a) schematic diagram, and (b) photos in operation

A total of 6 tests were performed at a centrifugal acceleration of 30g. Pull-out speed was kept constant at 0.2 mm/sec during all tests. This is equivalent to a pull-out speed of 0.007 mm/sec at prototype scale, which is sufficiently low to ensure fully drained behaviour (Bransby and Ireland, 2009). Fully saturated Fraction E sand (relative density I_D = 85%, saturated unit weight γ_{sat} = 19.4 kN/m^3) was used in all tests. The test programme and preliminary results are summarised in Table 4.

Table 4: Centrifuge test program (all values at model scale)

Test No.	Backfill	Saturated /Dry	H/D Ratio	Model Pipe Diameter (mm)
16	Sand	Saturated	0	8.7
17	Sand	Saturated	0.25	8.7
18	Sand	Saturated	0.5	8.7
19	Sand	Saturated	1	8.7
20	Sand	Saturated	2	8.7
21	Sand	Saturated	4	8.7

Results and Discussion

The recorded peak values of the "true" uplift resistance, R_{peak}, from all tests are summarized in Table 5. The back-calculated values for the effective soil weight, *W'*, vertical component of the shear force, *S*, and the Pederson Uplift Factor, f_p, based on Figure 2 and Equation 2 are also included. Centrifuge test data from Tests No. 16 to 21 have been converted to equivalent prototype values by employing scaling laws detailed in Schofield, (1980). Results from Tests No. 10 and 16 are omitted in the calculation of mean f_p values. This is not only because design scenarios with zero H/D ratio are rare, but also because the *W'* value in both tests is very small hence normalization based on it gives rise to amplified errors.

The best-fit f_p value for the first set of tests (Tests No. 1 to 7) is 0.67 with R^2 = 0.995. This f_p value and the minimum f_p value within this category can be inserted back into Equation 2, which produces best-fit and conservative predictions of R_{peak} respectively based on the Vertical Slip Surface Model. The same procedure have been carried out for the second (Tests No. 8 & 9), third (Tests No. 10 to 15), and fourth (Tests No. 16 to 21) test sets. The results are compiled in Figure 6, illustrating how the recorded test data fit with the two curves as well as the *W'* term which is the current design practice for H/D < 1.

Excellent agreement between recorded data and the predictions based on the Vertical Slip Surface Model is observed for all 21 tests. The back-calculated f_p values are higher than what DNV recommends (Table 1). However, the recorded distances that the pipe has to move upwards to mobilize R_{peak}, or mobilization distance, are much greater than what is specified in the DNV guideline. Hence the overall conservatism of the DNV design code is questionable.

The recorded R_{peak} values lie well over the *W'* curves throughout the whole H/D spectrum. Hence there is no evidence that the contribution from shear should be ignored when H/D ratio is less than 1. This conclusion should hold for uplift design scenarios in loose sand, dense sand and gravel. Interestingly, Tests No. 8 and 9 were carried out in exactly the same backfill conditions as Tests No. 1 to 7 except that the pipeline diameter is 2.5 times greater, yet the best-fit f_p values differ by 20%. This suggests that f_p could be related to the problem geometry as well as the intrinsic soil properties. More parametric studies are needed to draw definitive conclusions.

For uplift resistance in gravel, data seem to suggest that the shear component becomes reliable when the cover is at least 1-2 times the average particle diameter, D_{50}. Some representative force-displacement data are shown in Figure 7 for completeness.

Table 5: Summary of experimental results (all values at prototype scale)

Test No.	Backfill	H/D Ratio	D (mm)	R_{peak} (kN/m)	W' (kN/m)	S (kN/m)	S as % of R_{peak}	f_p	Mean f_p	Best-fit f_p	Min. f_p
1	Sand	0.1	100	0.052	0.018	0.034	65.36%	1.09			
2	Sand	0.3	100	0.095	0.036	0.059	61.83%	1.03			
3	Sand	0.4	100	0.115	0.044	0.071	61.67%	1.01			
4	Sand	0.5	100	0.130	0.053	0.077	59.40%	0.89	0.88	0.67	0.58
5	Sand	1	100	0.270	0.096	0.174	64.36%	0.89			
6	Sand	2	100	0.50	0.183	0.317	63.38%	0.58			
7	Sand	3.5	100	1.24	0.311	0.929	74.93%	0.68			
8	Sand	0.5	258	0.6	0.351	0.249	41.45%	0.43	0.51	0.56	0.43
9	Sand	1.0	258	1.4	0.641	0.759	54.25%	0.58			
10	Gravel	0	100	0.05	0.019	0.031	61.37%	0.68*			
11	Gravel	0.3	100	0.2	0.073	0.127	63.34%	1.12			
12	Gravel	0.5	100	0.3	0.109	0.191	63.56%	1.03			
13	Gravel	0.75	100	0.5	0.154	0.346	69.14%	1.23	1.17	1.31	1.03
14	Gravel	1	100	0.69	0.199	0.501	71.53%	1.11			
15	Gravel	2	100	1.9	0.379	1.521	80.04%	1.35			
16	Sand	0	258	0.385	0.068	0.317	82.21%	1.98*			
17	Sand	0.25	258	0.452	0.228	0.224	49.54%	0.62			
18	Sand	0.5	258	0.745	0.388	0.357	47.96%	0.56			
19	Sand	1	258	1.79	0.707	1.083	60.51%	0.75	0.65	0.68	0.62
20	Sand	2	258	3.8	1.345	2.455	64.60%	0.62			
21	Sand	4	258	11.5	2.622	8.878	77.20%	0.69			

* Results from Tests No. 10 and 16 are omitted from Mean, Best-fit and Minimum f_p calculations as W' value in both tests is very small and f_p in these tests are outliers.

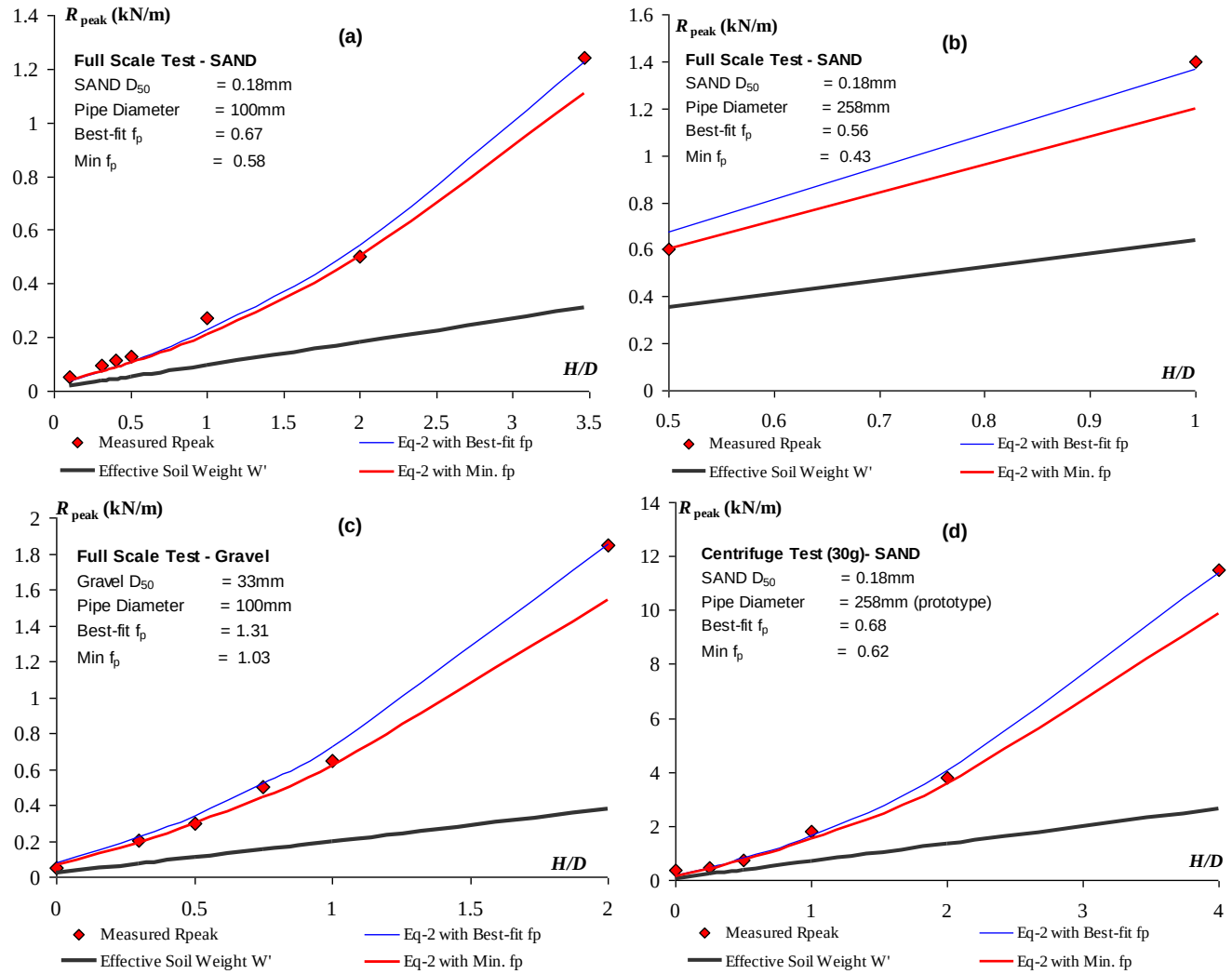

Figure 6: Recorded R_{peak} data compared with predictions from Equation 2 for (a) Tests No. 1 to 7; (b) Tests No. 8 & 9; (c) Tests No. 10 to 15; and (d) Tests No. 16 to 21

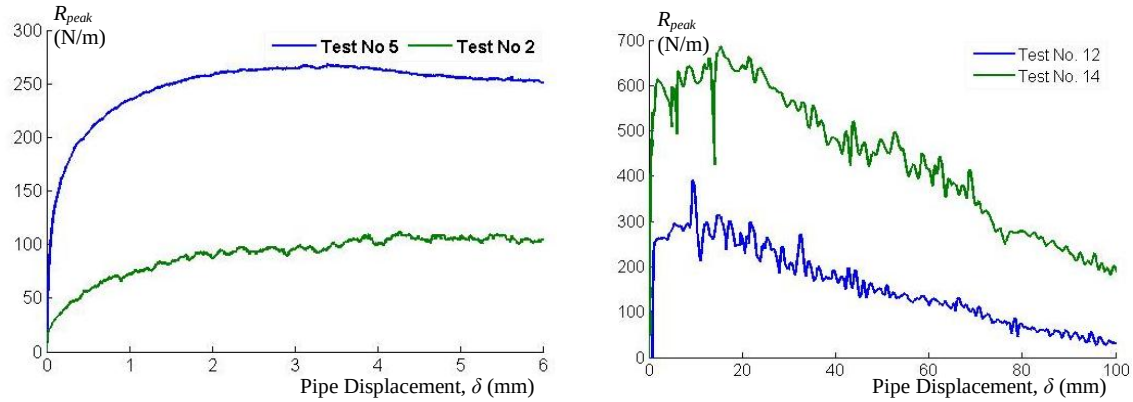

Figure 7: Representative uplift force-displacement test data

Uplift Mechanism from Particle Image Velocimetry (PIV)

For Tests No. 1 to 9, the soil displacement field during the uplift event was accurately measured at 5-second intervals, which corresponds to 0.025 mm of upward displacement by the model pipe. This was achieved using the non-contact digital image correlation technique of particle image velocimetry (PIV), described in detail by White, (2002), Take, (2003), and White et al., (2003). PIV operates on the visual image texture of the soil (colour, grain orientation, etc.), which allows the precise determination of soil displacements though a series of digital images without resorting to predefined target markers. The displacement field can subsequently be analysed to produce the corresponding strain field, which illustrates the deformation mechanism in an intuitively visible manner.

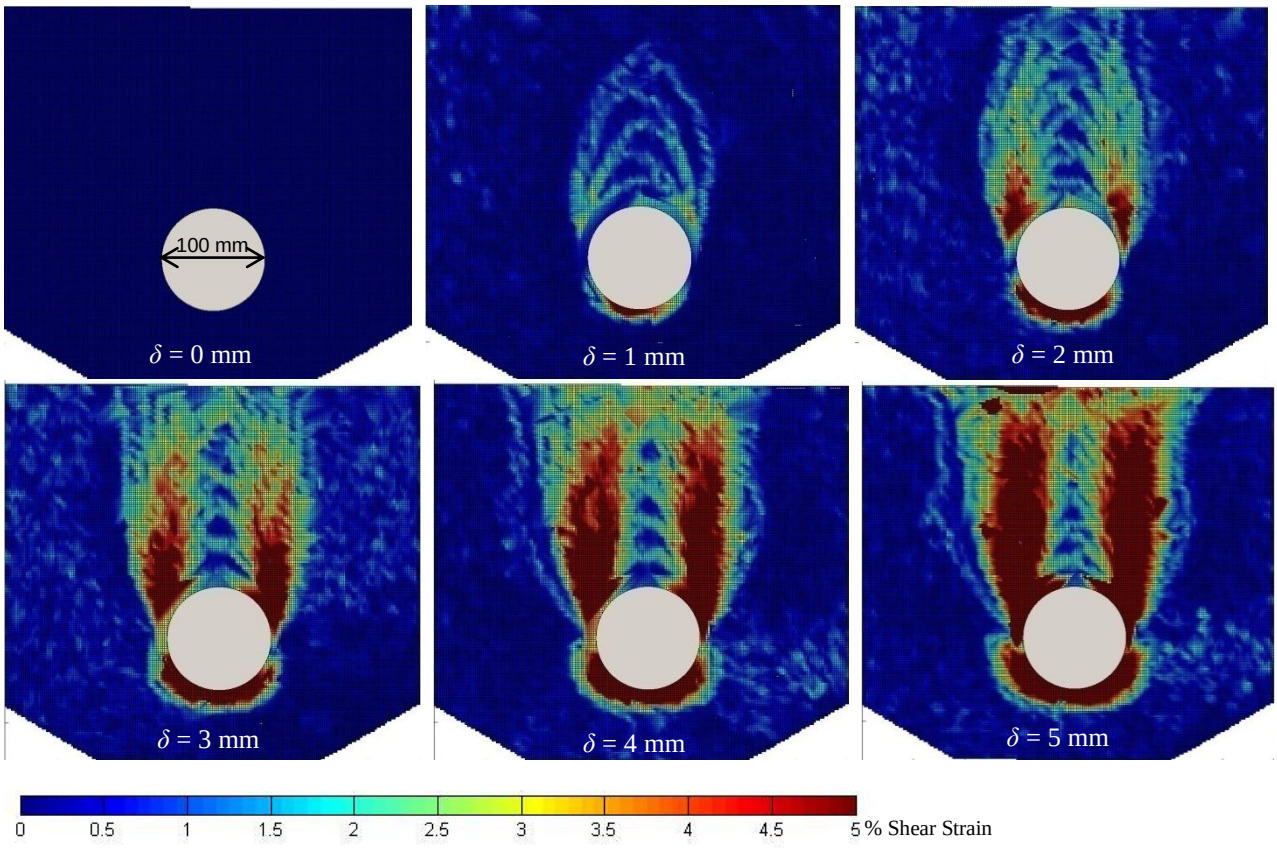

Figure 8: Evolution of total shear strain for Test No. 6

As an example, the evolution of soil shear strain with pipe upward displacement for Test No. 6 (H/D = 2) is illustrated in Figure 8. It is clearly visible that the uplift mechanism in loose sand can be divided into three phases:

1. At very small displacements (δ < 1 mm in this case), thin strands of compression fronts (interpreted as shear bands in total shear strain plots) originate from one side of the pipe crown, fanning out gradually to the other side and swiftly propagating through the backfill soil medium. Localised dilation shear zones start to appear

underneath the pipe, which ultimately creates a wedge-shaped void.

2. At small pre-peak displacements (1 mm < δ < 4.6 mm in this case), propagation becomes slower and slower and almost comes to a standstill when these compression fronts have rotated over 90 °. Subsequent compression fronts start to superimpose on their predecessors. Two cumulated macroscopic shear bands of more than 5% total shear strain originate from both edges of the pipe crown, and start to propagate almost vertically towards the soil surface. New-born compression fronts start to converge on and merge into the two macroscopic shear bands. R_{peak} is usually reached when this macroscopic shear band just reaches the soil surface.
3. At post-peak displacements (δ > 4.6 mm in this case), the existing mechanism reinforces itself, and the two macroscopic shear bands start to move sideways and widen in a very gradual manner.

The widths of both the smaller compression fronts and the bigger macroscopic shear bands seem independent of the H/D ratio. At peak uplift resistance, the centre lines of the two shear bands coincide very well with the two shear planes specified in the Vertical Slip Surface Model. Hence, PIV strain analysis verifies that this model is a good representation of the true uplift deformation mechanism in loose sand at low to medium H/D ratios.

At very low H/D ratios (H/D < 0.5), the macroscopic shear bands would form a wedge instead of a vertical column at R_{peak}, as illustrated in Figure 9. This is likely a result of reduced difficulty for compression fronts to propagate laterally when cover is small. As a result, more soil is being lifted than what is assumed by the Vertical Slip Surface model. However, this extra contribution from the effective soil weight term is compensated by the reduction in the shear forces due to reduced normal stress on the two inclined shear planes compared with the vertical case. Hence the overall deviation from the predicted values using Equation 2 is likely to be small.

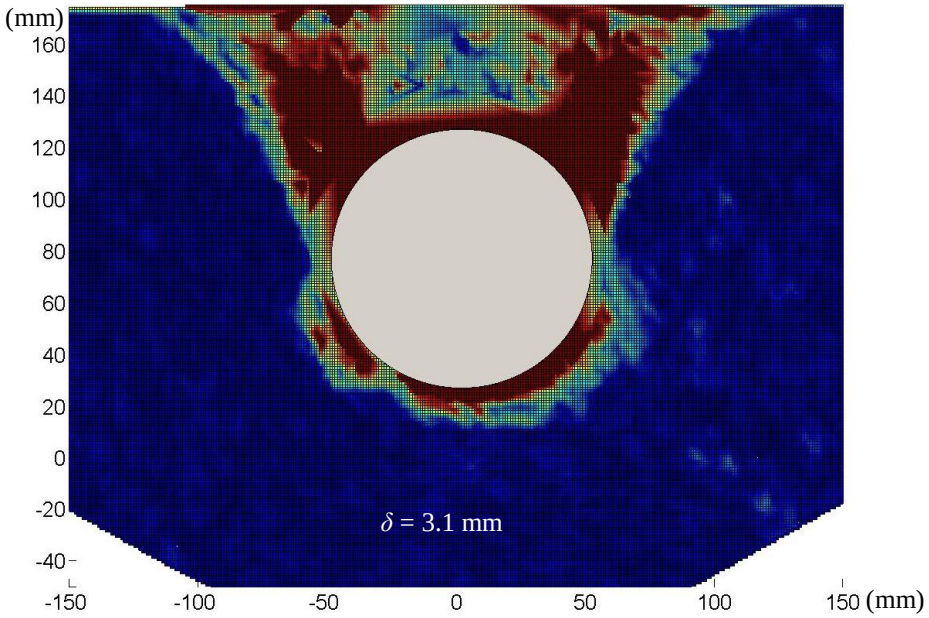

Figure 9: Total shear strain plot at R_{peak} for Test No. 3 (H/D = 0.4)

PIV strain analysis also provides useful insight into the width of the influence zone above the soil surface during the uplift event. In loose sand, the width of this influence zone seems to be approximately 2.5 times the pipeline external diameter. Hence if additional downward force is to be provided by rock dump, the width of dumping should be of similar dimensions to ensure maximum efficiency.

Note on Mobilization Distance

In order to fully mobilise the maximum "true" uplift resistance R_{peak}, the pipeline has to move upwards by a minimum distance. Underestimation of this mobilization distance is equivalent to overestimation of the available uplift resistance at small displacements. Hence, Equation 2 must be used in conjunction with a reliable estimate of the mobilization distance in order to produce a truly safe design guideline. The uplift force-displacement curves for all 21 tests as well as other available data in literature have been normalized to derive how mobilization distance varies with H/D ratios, pipe diameter, and various other parameters. Mobilization distance in uplift resistance design is explained in more detail in Thusyanthan et al., (2010) and Wang et al., (2010).

For further analyses and conclusions on the interaction of mobilization distance and R_{peak}, please refer to Wang, Haigh, and Thusyanthan (2010).

Conclusions

The reliability of the shear force contribution towards the maximum "true" uplift resistance at low H/D ratios is assessed, with a particular focus on H/D ratios below 1. A series of pipeline uplift resistance tests have been devised and conducted in cohesionless soils at the Schofield Centre, University of Cambridge. These tests can be subdivided into three categories:

1. Full scale (1g) uplift resistance testing in loose saturated sand (9 tests, covering H/D ratios from 0.1 to 3.5)
2. Full scale (1g) uplift resistance testing in dry gravel (6 tests, covering H/D ratios from 0 to 2)
3. Centrifuge (30g) uplift resistance testing in dense saturated sand (6 tests, covering H/D ratios from 0 to 4)

Excellent agreement between recorded R_{peak} data and the corresponding values predicted by the Vertical Slip Surface Model is observed in all 21 tests. The recorded R_{peak} values lie well over the W' curves throughout the whole H/D spectrum. There is no evidence that the contribution from shear should be ignored when H/D ratio is less than 1. Hence the Vertical Slip Surface Model and the associated design equation are still applicable for design scenarios with H/D ratios less than 1. Based on available test data, this conclusion should hold for uplift resistance design in loose sand, dense sand and gravel. For uplift resistance in gravel, the shear component becomes reliable when the cover is at least 1-2 times the average particle diameter. This suggests that the current design practice is overly conservative in predicting R_{peak} values when H/D is less than 1. However, the uplift force-displacement data also suggests that the DNV code underestimates the mobilization distance, which could lead to unsafe design despite the over-conservatism on R_{peak}.

The Particle Image Velocimetry (PIV) technique has been adopted to reveal the soil deformation mechanism during the uplift event. Results from total shear strain field analyses have demonstrated that the Vertical Slip Surface Model is a good representation of the true uplift deformation mechanism in loose sand. The evolution of shear strain field also provides useful insight into how uplift resistance is gradually mobilized as the uplift event progresses.

Acknowledgement

The authors would like to thank all staff at the Schofield Centre, University of Cambridge for their help and advice throughout the testing program. The first author would also like to thank Trinity College, University of Cambridge, and KW Ltd. for their generous financial support towards this research effort.

References

Barker, H.R. (1998). Physical modelling of construction process in the mini-drum centrifuge. *PhD Dissertation*, University of Cambridge.

Baumgard, A.J. (2000). Monotonic and cyclic soil response to upheaval buckling in offshore buried pipelines. *PhD Thesis.* University of Cambridge.

Bransby, M.F. and Ireland, J. (2009). Rate effects during pipeline upheaval buckling in sand. *Geotechnical Engineering* **162**: 247-256.

Bransby, M.F., Newson, T.A., Brunning, P., and Davies, M.C.R. (2001). Numerical and centrifuge modelling of upheaval resistance of buried pipelines. *Proc. OMAE*, Rio de Janeiro, June 2001.

Cheuk, C.Y. (2005). Soil pipeline interaction at the seabed. *PhD thesis.* University of Cambridge.

Croll, J.G.A. (1997). A simplified model of upheaval thermal buckling of subsea pipelines. *Thin-Walled Structures* **29** (1-4): 59-78.

Dickin, E.A. (1994). Uplift resistance of buried pipelines in sand. *Soils and Foundations* **34** (2): 41-48.

DNV-RP-F110, Global buckling of submarine pipelines – structural design due to high temperature / high pressure. *Det Norske Veritas*, Norway, 2007.

Hobbs, R. (1984). In service buckling of heated pipelines. *ASCE Journal of Transportation Engineering* **110** (2): 175-189.

Moradi, M. and Craig, W.H. (1998). Observations of upheaval buckling of buried pipelines. *Centrifuge 98*, Kimura, Kusakaba & Takemura (eds), ISBN 90 5410 986 6

Palmer, A.C., Ellinas C.P., Richards, D.M., and Guijt, J. (1990). Design of submarine pipelines against upheaval buckling. *Proc. Offshore Technology Conf., Houston*, OTC 6335: 551-560.

Palmer, A.C. White, D.J., Baumgard, A.J., Bolton, M.D., Barefoot, A.J. Finch, M., Powell, T., Faranski, A.S., Baldry, J.A.S. (2003). Uplift resistance of buried submarine pipelines: comparison between centrifuge modeling and full-scale tests. *Géotechnique* **53** (10): 877–883

Pedersen, P.T. & Jensen, J.J. (1988). Upheaval creep of buried pipelines with initial imperfections. *Marine Structures* **1**:11-22, 1988.

Randolph, M. F., & Houlsby, G. T. (1984). The limiting pressure on a circular pile loaded laterally in cohesive soil. *Géotechnique*, **34** (4): 613-623.

Rowe, R.K., and Davis, E.A. (1982). The behaviour of anchor plates in sand. *Géotechnique* **32** (1): 25-41.

Schaminée, P.E.L., Zorn, N.F., and Schotman, G.J.M. (1990). Soil response for pipeline upheaval buckling analysis: Full-scale laboratory tests and modelling. *Offshore Technology Conference*, Houston, OTC 6486

Schofield, A.N. (1980). Cambridge Geotechnical Centrifuge Operations. *Géotechnique* **30** (3): 227-268.

Take, W.A. (2003). The influence of seasonal moisture cycles on clay slopes. *PhD dissertation*, University of Cambridge, UK.

Timoshenko, S. and Goodier, J. N. (1934). Theory of Elasticity. McGraw-Hill Book Company.

Thusyanthan, N. I., Ganesan S. A & Bolton M.D. and Peter Allan (2008). Upheaval buckling resistance of pipelines buried in clayey backfill. *Proceeding of ISOPE 2008, The Eighteenth (2008) International Offshore and Polar Engineering Conference*, Vancouver, Canada, July 6 - 11, 2008

Thusyanthan, N.I., Mesmar, S., Wang J., and Haigh, S.K. (2010). Uplift resistance of buried pipelines and DNV-RP-F110 guideline. *Proc. Offshore Pipeline and Technology Conference*. Feb 24-25, Amsterdam, Netherlands.

Trautman, C.H., O'Rourke, T.D., and Kulhawy, F.H. (1985). Uplift force-displacement response of buried pipe. *ASCE Journal of Geotechnical Eng. Division* **111** (9): 1061-1075.

Vesic, A.S. (1971). Breakout resistance of objects embedded in ocean bottom. *ASCE Journal of the Soil Mechanics and Foundation Division*.**97** (9): 1183-1205.

Wang, J., Haigh, S.K., and Thusyanthan, N.I. (2009). Uplift resistance of buried pipelines in blocky clay backfill. *Proc. International Offshore (Ocean) and Polar Engineering Conference*. ISOPE 2009 TPC 564.

Wang, J., Haigh, S.K., Thusyanthan, N.I., and Mesmar, S. (2010). Mobilisation distance in uplift resistance modeling of pipelines. *Proc. International Soposium on Frontiers in Offshore Geotechnics.* Nov. 8-10, 2010, Perth, Australia.

Wang, J., Haigh, S.K., and Thusyanthan, N.I. (2010). Uplift resistance design of shallowly buried pipelines. *ASCE Pipelines Journal* (currently being drafted).

White, D.J., Barefoot, A.J., Bolton, M.D. (2001). Centrifuge modelling of upheaval buckling in sand. *International Journal of Physical Modelling in Geotechnics*, **2** (1):19-28.

White, D.J. (2002). An investigation into the behaviour of pressed-in piles. *PhD dissertation*, University of Cambridge, UK.

White, D. J., Take, W. A. & Bolton, M. D. (2003). Soil deformation measurement using particle image velocimetry (PIV) and photogrammetry. *Géotechnique*, **53** (7): 619–631.